# NUMERICAL SIMULATION OF CURRENTS GENERATED BY HURRICANES.

CORTIS COOPER
*New England Coastal Engineers, Inc.*
*Bangor, Maine, U.S.A.*

GERMÁN FEBRES ORTEGA & JOSÉ L. PELEGRI
*Departamento de Ingeniería General*
INTEVEP, S. A.

ABSTRACT: A 3-dimensional numerical circulation model has been under development for INTEVEP during the past 3 years. The objective has been to obtain a state-of-the-art model to predict storm-induced currents along the Venezuelan Coast. Results are to be used, in part, to determine design currents for offshore petroleum development. This paper briefly describes the theoretical basis of the model, known as GAL, as well as applications to Tropical Storm Delia and Hurricanes Flora and Anita. Current data was recorded for Anita and Delia in the Gulf of Mexico. The model is used to hindcast the currents from these two storms in order to: (a) gain insight into the physical processes which govern the two somewhat empirical coefficients used into the model and (b) evaluate the model's capability for simulating storm induced currents. The hindcast results give some interesting and valuable insight into the processes affecting the two coefficients as well as the currents in general. The validity and usefulness of the model is clearly established.

RESUMEN: Un modelo numérico tridimensional de circulación ha venido siendo desarrollado para INTEVEP durante los tres últimos años. El objetivo ha sido obtener un modelo avanzado capaz de predecir corrientes ocasionadas por tormentas a lo largo de la Costa Venezolana. En parte, los resultados deberán ser usados para determinar valores de diseño de corrientes para el desarrollo petrolero costa afuera. Este artículo describe brevemente la base teórica del modelo conocido como GAL, así como su aplicación para la Tormenta Tropical Delia y los Huracanes Flora y Anita. Datos de corrientes fueron registrados para Anita y Delia en el Golfo de México. El modelo es usado para predecir las corrientes ocasionadas por estas dos tormentas con el propósito de: (a) dar mayor claridad a los procesos físicos que gobiernan a los dos coeficientes semiempíricos usados en el modelo y (b) evaluar la capacidad del modelo en la simulación de corrientes producidas por tormentas. Las predicciones dan interesantes y valiosos aportes a los procesos que afectan los dos coeficientes, así como sobre las corrientes en general. La validez y utilidad del modelo es claramente establecida.



## 1. INTRODUCTION

The circulation model described in this paper has been developed to provide information about the temporal and spatial variations of the horizontal velocities, while at the same time being economical to operate. Extensive testing and comparisons of the model to analytic solutions have verified both the convergence and the stability of the numerical scheme. These comparisons, along with a more complete description of the formulation, appear in Pearce and Cooper (1). Only a brief explanation of the model formulation is included in this paper. The applications described herein are the hindcasting of currents for Tropical Storm Delia and Hurricane Anita. Preliminary hindcast results are found for Tropical Storm Delia in Pearce *et al.* (2). The data for Tropical Storm Delia originated from Forristall, Hamilton, and Cardone (3), henceforth refered to as FHC. Data were recorded on the Buccaneer platform in the Gulf of Mexico. Buccaneer was equipped with three electromagnetic current meters, barometer, and wind sensor. The storm center of Delia passed within a few kilometers of Buccaneer and produced a minimum pressure of 987 mb, a peak wind gust of 32 m/s and extreme waves of

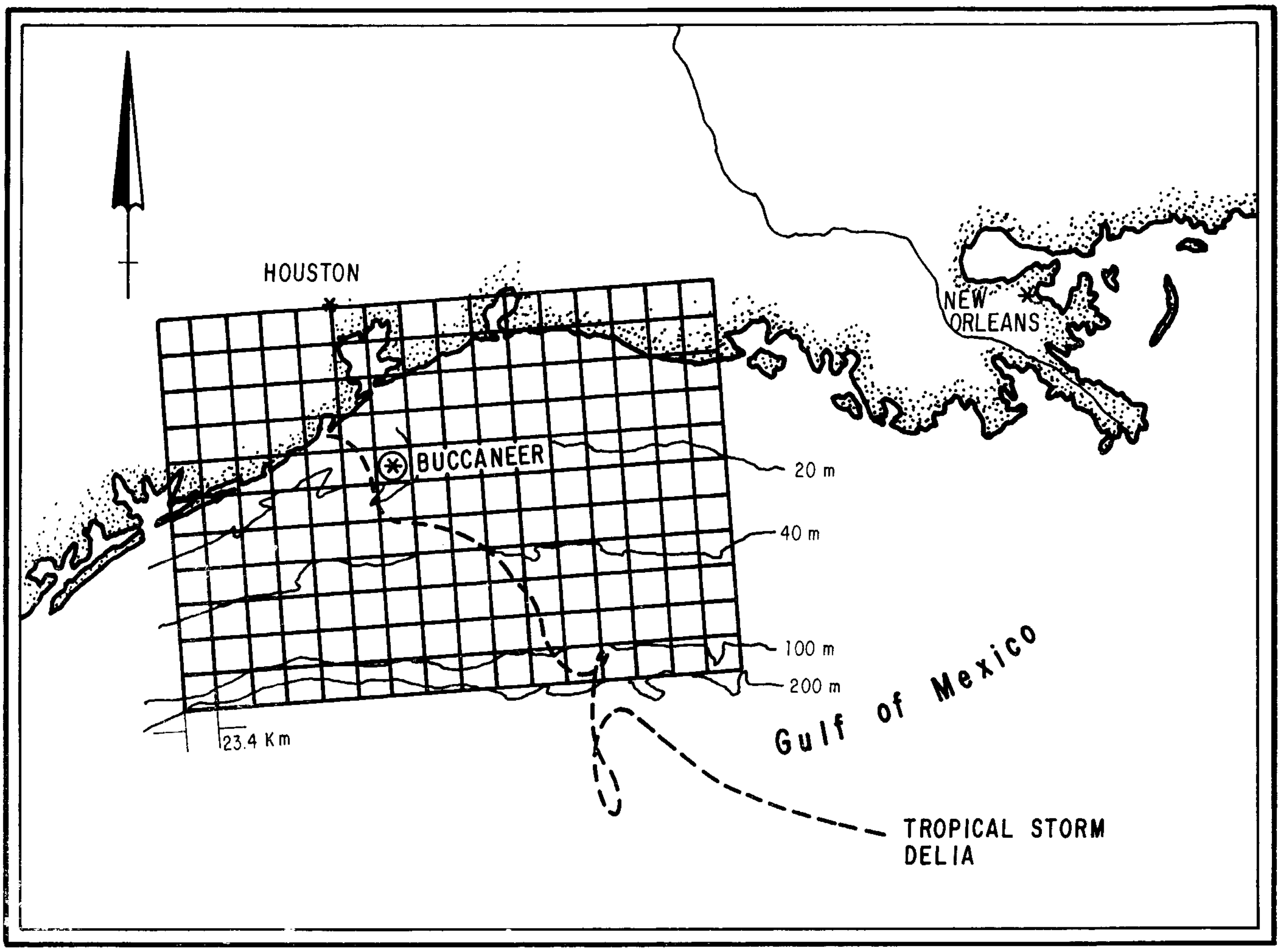


Fig. 1. Location of Buccaneer Platform and storm track for Tropical Storm Delia. Also shown is the grid initially used in the wind and circulations models (from Pearce *et. al,* (2) ).

7-8 m. Figure 1 shows the location of Buccaneer and the storm track, as well as the grid system initially used in the wind and current models.

Hurricane Anita occurred in September 1977 and passed through the Northern Gulf of Mexico. Data were reported by Smith (4). Current data were taken at a site about 20 km off the Texas Coast in about 17 m of water (see Figure 2). Two current meters were deployed, one at 7 m below still water level and another at 15 m. The nearest wind data were recorded at Port Aransas, Texas, about 120 km from the site of the current meters. The center of the storm passed within 360 km of the current meter site, creating maximum currents of about 1 m/s. Maximum winds recorded at Port Aransas were 48 km/hr.

The purpose of the simulations presented here is to: (a) gain insight into the physical processes which govern the two, somewhat empirical, coefficients used in GAL and (b) evaluate GAL's capability to simulate storm currents. It has not been possible to perform the above studies with storm data from the Venezuelan Coast. There is simply no historical current data recorded during storm conditions. One of the principal reasons for the recent data collection programs undertaken by INTEVEP along the Venezuelan coast has been to record data during tropical storm events, but unfortunately storm data along the coast are still lacking. Until that data are obtained, it is neccesary to test and verify the model using data from other locations. Given the strong theoretical and physical basis of the model, it is expected that the simulations performed in other locations will still be quite useful and can be utilized

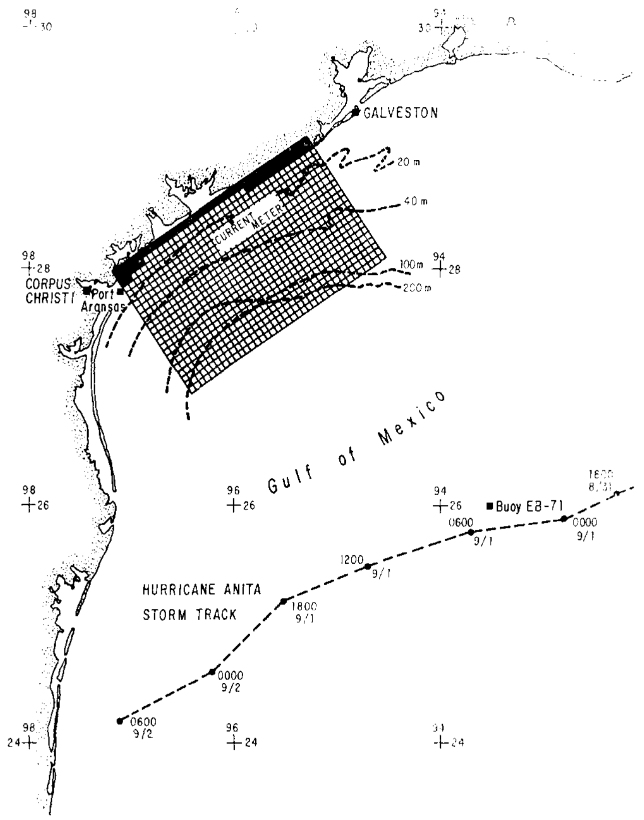


Fig. 2. Location of the current meters and storm track for Hurricane Anita. Also shown is the grid used in the wind and circulation models.

to predict design currents along the Venezuelan coast. When storm data are eventually recorded along the Venezuelan coast it will be used to further refine the model and design currents.

## 2. WIND MODEL

Due to the lack of synoptic wind data it was necessary to use a wind model. The simple wind model used to provide the necessary atmospheric inputs to the circulation model incorporates a symmetric pressure field suggested by Harris (5). The wind field was modeled using relationships reported by Stone and Webster (6) and attributed to Jelesnianski (7). The equations used in the wind model are given in Pearce *et al.* (2).

Use of the wind model requires specification of the deflection angle, radius to maximum winds, temporal variation of storm position and central and peripheral pressure.

### 2.1. *Delia wind simulation*

Wind data from Tropical Storm Delia are published in FHC in two forms: the wind velocity and pressure as recorded at Buccaneer, and the central pressure measured by the Air Force and Navy. Data are not available for the radius to maximum winds although FHC suggest a value of 65 km based on occurrence of maximum wind at Buccaneer and Galveston, Texas. In the process of tuning the wind model used in this study, it was found that the best comparisons at Buccaneer were obtained when the radius to maximum winds was varied between 85 km and 64 km during the course of the storm.

The deflection angle is often treated as a constant; however, Myers and Malkin (8) compiled observed data which suggest that, in fact, the deflection angle displays significant temporal and spatial variability for a particular storm. Since there was no synoptic wind data, measurements of the deflection angle are not available. Hence, in the wind field modeling of Delia, the deflection angle was treated as a tuning parameter and varied to yield the best comparison between the wind data and the model. An angle of 5° was found to simulate best the measured data.

The shear relationship used to couple the wind model with the circulation model is taken from Wu (9). Wind shear stresses, pressure gradients and the so-called inverted barometer effect were passed from the wind model to the circulation model on an hourly basis. FHC used somewhat more sophisticated wind and shear stress relationships than those used in this study. The models used by FHC were based on work done by Cardone *et al.* (10) and Cardone (11). Cardone's expression for the shear stress indicates that the drag coefficient varies approximately the same as Wu's in the range from 5 m/s to 20 m/s.. Above the latter value, however, Wu's formulas specify the drag coeficient to be constant, whereas Cardone's expression indicates that the drag coefficient increases linearly with speed (for neutral stability). Since wind speeds in Delia were never greater than about 25 m/s, the two shear stress relationships behave in essentially the same manner.

A comparison of the modeled winds and observed winds at Buccaneer is shown at the bottom of Figure 4. Note that the winds are broken into two components: an alongshore (positive in an easterly direction) and a cross-shelf component (positive in a northerly direction).

### 2.2. *Anita Wind Simulations*

Modeling of the winds proceeded in a manner very similar to that used for the Delia simulation. The wind model by Jelesnianski was used and the input parameters were varied to achieve the best comparisons between observed wind speeds at Port Aransas and simulated wind speeds. A comparison between the final simulated winds and the observed winds is given in Figure 5. Also shown are the modeled winds at the current meter site.

Note that winds are broken into two components: an alongshore component and a cross-shelf (or onshore/offshore) component. The alongshore component is aligned with the axis of the grid (see Figure 2), oriented in a northeast-southwest direction. A positive sign indicates winds from the northeast direction. The cross-shelf component is positive when winds are from the north-west direction.

To simulate winds at such a great distance from the storm center using the simple Jelesnianski model, it was necessary to use somewhat unrealistic values for the deflection angle. The angle was varied between approximately + 30° to — 30°. A more accurate description of the wind could be obtained using a more sophisticated wind model, but in light of the absence of other wind data, use of a more sophisticated model was not felt to be justified.

## 3. CIRCULATION MODEL

The model, GAL, which was used to hindcast the current data, takes its name from the Galerkin numerical technique upon which the model is based. Model formulation is founded on the description of the vertical variation of the horizontal velocity by a series expansion (see Heaps, (12), (13) ). A thorough description of the model is included in Pearce and Cooper (1). Only a brief description will be given in this paper.

The model is bassed on the Navier Stokes Equations which, after some simplifying assumptions, can be written in the form used in the model as:

$$0 = \frac{\partial u}{\partial t} + \frac{\rho_s}{\rho} g \frac{\partial \eta}{\partial x} - \epsilon u - \frac{\partial}{\partial z}\left(N_v \frac{\partial u}{\partial z}\right) - fv + \frac{1}{\rho}\frac{\partial P_a}{\partial x} + \frac{g}{\rho}\int_{-\eta}^{z} \frac{\partial \rho}{\partial x}\, d\zeta$$

$$0 = \frac{\partial v}{\partial t} + \frac{\rho_s}{\rho} g \frac{\partial \eta}{\partial y} - \epsilon v - \frac{\partial}{\partial z}\left(N_v \frac{\partial v}{\partial z}\right) + fu + \frac{1}{\rho}\frac{\partial P_a}{\partial y} + \frac{g}{\rho}\int_{-\eta}^{z} \frac{\partial \rho}{\partial y}\, d\zeta \qquad (1a,b)$$

where

t — the time variable.

x,y — the horizontal coordinates in a rigth-handed Cartesian coordinate system.

z — the vertical coordinate, measured as positive downward from the still water surface.

u,v — the horizontal velocity components in the x and y directions, respectively.

$\rho_s$ — the density of the fluid, where the s subscript indicates the value at the surface.

g — the gravitational constant, 9.8 m/s$^2$

$\eta$ — the water height of the free surface above datum, z = 0.

$\epsilon$ — a constant simulating the lateral shear stress terms. The Guldberg-Mohn (14) assumption is applied.

$N_v$ — the vertical eddy viscosity coefficient.

f — the Coriolis parameter, $2\omega\sin\Phi$, where $\omega$ is the velocity of the earth and $\Phi$ is the latitude.

$P_a$ — the atmospheric pressure.

Note that the vertical velocity, w, is assumed negligible and this simplifies the Navier Stokes Equation in the z direction to an expression of the hydrostatic pressure. The density gradient terms, lateral shear stress terms, and the tidal components were neglected in the simulations. This was felt justified given the strong winds which dominated the region during the storm.

The other governing equation used in the model formulation is the continuity equation:

$$\frac{\partial \bar{U}}{\partial x} + \frac{\partial \bar{V}}{\partial y} = \frac{\partial \eta}{\partial t} \qquad (2)$$

where

$\bar{U}$ — the mass flux per unit length in the x direction or $\int_{-\eta}^{H} u\,dz$.

$\bar{v}$ — the mass flux per unit length in the y direction or $\int_{-\eta}^{H} v dz$.

The surface boundary conditions are:

$$\tau_{sx} = \{-\rho N_v \frac{\partial v}{\partial z}\} \Big|_{z=0}$$
$$\tau_{sy} = \{-\rho N_v \frac{\partial u}{\partial z}\} \Big|_{z=0} \qquad (3)$$

vhere $\tau_{sx}$ and $\tau_{sy}$ are the specified shear stresses at the surface in the x and y direction respectively

At the bottom, a linearized friction law is used

$$\tau_{bx} = \{-\rho c_b u\} \Big|_{z=H}$$
$$\tau_{by} = \{-\rho c_b v\} \Big|_{z=H} \qquad (4)$$

where $\tau_{bx}$ and $\tau_{by}$ are the bottom shear stresses, H is the still water depth, and $c_b$ is the drag coefficient.

The remaining boundary conditions vary somewhat according to the water body being modeled. The following lateral boundary conditions were assumed for the simulations:

a) the mass fluxes perpendicular to a coastline were set to zero;
b) the surface gradient perpendicular to a lateral ocean boundary was set to zero (a lateral boundary is defined as the boundary running from deep water to the shoreline); and
c) the amplitude at all open ocean boundaries was set equal to the barometrically - induced water rise (i.e. the "inverted barometer effect").

It is important to note that the parameters u, v, $\rho$, and $N_v$ are all functions of space and time (x, y, z, t), and the parameters $\epsilon$, $\eta$, $c_b$, and $P_a$ are functions of horizontal space and time (x, y, and t). Parameters which must be specified are $\rho$, $N_v$, f, $P_a$, $c_b$, $\tau_{sx}$, $\tau_{sy}$, and $\epsilon$, and the unknowns are u, v, and $\eta$.

The governing equations and boundary conditions (i.e., equations 1, 2, 3, and 4) are transformed using the Galerkin technique. This manipulation explicitly eliminates z from the transformed equations and thus greatly simplifies the eventual solution process. The dependency of u and v on z is implicity retained in the final equations and the u and v velocity profiles can be regained whenever desired.

Application of the Galerkin technique begins by hypothesizing a vertical distribution of the unknown velocities, u and v, in terms of a series expansion known as the trial function. The function used in the model is

$$u = \frac{\tau_{sx} z^2 (z-H)}{\rho_s H^2 N_b} - \frac{\tau_{sx}}{\rho . \alpha} \ln \left(\frac{N_b}{N_v}\right) + \sum_{I=1}^{I=I'} C_I \cos \left(\frac{a_I z}{H}\right) \qquad (5)$$

where

$\hat{u}$, $\hat{v}$ — approximate x and y components of the velocity, respectively
$N_b$ — vertical eddy viscosity at the bottom, z = H.
$\alpha$ — slope of $N_v$ in the surface layer
I' — number of terms used in the cosine series.
$a_I$ — constants given by the expression $a_I \tan a_I = \frac{C_b H}{N_b}$
$c_I$ = the undetermined constants

A similar function exists for $\hat{v}$. The relationships for the y-direction will not be shown in this paper for the sake of brevity. However, the reader should remember that these equations are included in the model. Note that all parameters in (5) are specificied except the undetermined coefficients, $c_I$ (for the y-direction the undetermined coefficients are $d_I$).

The trial functions are substituted into (1a, b) and, in general there will be an error or residual associated with this substitution since the trial functions are not the exact solutions. The residual, R, is multiplied by a weighting factor, W, to facilitate later computation and the product is minimized by integrating over the water depth and setting the result to zero, or for the x-direction:

$$\int_{-\eta}^{H} RWdz = \int_{-\eta}^{H} \left(\frac{\partial \hat{u}}{\partial z} + \frac{\rho_s}{\rho} g \frac{\partial \eta}{\partial x} - \epsilon \hat{u} + \frac{1}{\rho} \frac{\partial P_a}{\partial x} + \frac{g}{\rho} \int_{-\eta}^{Z} \frac{\partial \rho}{\partial x} d\zeta \right) \cos \frac{a_I z}{H} dz = 0 \qquad (6)$$

Again, a similar expression exists for the y-direction.

Before the integration in (6) can be performed, it is necessary to specify a vertical distribution for $N_v$. This is accomplished by assuming $N_v$ to vary in a multi-linear fashion as shown in Figure 3.

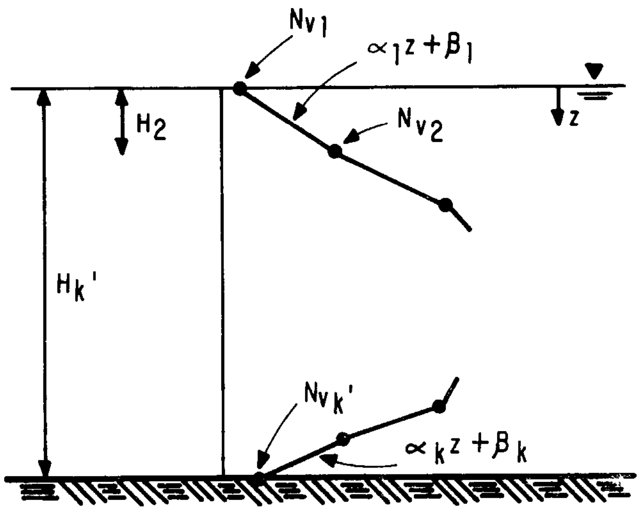


Fig. 3. Functional form for the vertical variation of $N_v$.

Performing the integration in (6) yields a set of I' linear partial differential equations in which z has been explicitly eliminated or

$$0 = \frac{\partial c_I}{\partial t} - \epsilon c_I - fd_I + B_I \frac{\partial \eta}{\partial x} + A_I - \sum_{J=1}^{J=I'} c_J E_{IJ} \tag{7}$$

where $A_I$, $B_I$, and $E_{IJ}$ are constants which arise from the integration.

Equation 7 and its equivalent in the y-direction represent a set of 2I' equations with 2I' + 1 unknowns (i.e. $c_I$, $d_I$ and $\eta$). To solve for the unknowns one more equation linking $c_I$ $d_I$, and $\eta$ mut be used, and this is provided by substituting (5) into the continuity equation (2).

The existing version of the model uses a finite difference scheme to discretize (7), its equivalent in the y-direction, and the transformed continuity equation. While this discretization scheme has proven satisfactory it is not limiting since other schemes such as finite elements could be used.

The key in applying the Galerkin technique is in choosing the initial trial functions, (5). In order for the model scheme to simulate the velocity structure economically and accurately, (5) must be able to converge rapidly to the vertical velocity profile being modeled. Equation (5) has proven to be quite adequate in this regard. Usually only three cosine terms (i.e. I' = 3) have proven necessary for the wide variety of flow fields simulated thus far. Some of these applications have included wind-induced flow which is often characterized by large velocity gradients near the surface. Such flow fields cannot be adequately simulated by many existing models including Heaps' model. In large part due to (5), the model has proven computationally economical, cost being about the same as for a vertically-averaged model (e.g. Wang and Connor, (15) or Weare, (16) ).

## 4. HINDCASTS OF CURRENTS FOR TROPICAL STORM DELIA

Preliminary application of the model to the FHC data set is described in Pearce *et al.* (2). Since publication of that paper, work has progressed and the comparisons presented in this paper are somewhat better and more thorough than those described above. The grid size used in the final simulations presented here was 20 elements long by 32 elements wide and was basically the same as the initial grid shown in Figure 1 except that the resolution was doubled (i.e. element size = 11.7 km).

The current data described by FHC were obtained from three electromagnetic current meters fixed at 4, 10, and 19 meters below still water level. Still water depth at the platform was 20 m and Buccaner was located about 50 km from the nearest coastline. Wind velocity was recorded on the platform at a height of 30 m above mean water. Pressure data was taken on the platform and by the Air Force and Navy. Wind velocities were calculated hourly and details of the wind modeling are included in Section 2.

The choice of the vertical eddy viscosity, $N_v$, and bottom friction coeficient, $c_b$, used in the model is important and yet there is little theoretical foundation upon which to base a choice, especially in the presence of large waves. Thus, although the model has the capability of including a vertical variation in $N_v$, it was decided to assume it to be constant in the vertical given the lack of data concerning $N_v$ in storm conditions.

### 4.1 *Estimates of* $c_b$

Estimates for $c_b$ can be obtained by relating $c_b$ to a quadratic bottom friction coefficient such as Manning's n:

$$C_b = \frac{n^2 u_b g}{(H)^{1/3}} \qquad (8)$$

where $u_b$ is the velocity at the bottom ($Z = H$), and the units are in the MKS system. To estimate n, one must estimate the sea floor condition near Buccaneer. FHC indicate that the bottom is smooth clay at Buccaneer, as one might expect for the Delta region of the Gulf of Mexico. Hydraulic experiments show a range of values for n between 0.017 and 0.027 for "straight and uniform earth" (e.g. Daily and Harleman, (17) ). Using a nominal value for $n = 0.0225$, a mean value of $u_b = 1$ m/s and $H = 20$ m yields from (8), $c_b = 0.0019$ m/s which compares reasonably well to the value of $c_b = 0.0010$ m/s which was found to give the best overall comparison between the modeled and observed velocity profiles at Buccaneer. FHC also used a value of 0.0010 m/s for $c_b$ in their simulations.

### 4.2 *Estimates of* $N_v$

Estimates of $N_v$ are difficult at best and are even more so for relatively strong wind events such as Delia. Neumann and Pierson (18) report a number of studies estimating $N_v$. All these expressions relate $N_v$ either to wind speed or to wind speed and latitude. Studies by Schmidt (19), Thorade (20) and Neumann (21) appear to be most appropriate for the Delia case and agree reasonably well, indicating $N_v = 0.2$ m²/s for wind speeds of 24 m/s (peak winds during Delia). However, this predicted value compares poorly to some of the other values reported in Neumann and Pierson, and is nearly an order of magnitude larger than the value of $N_v = 0.03$ m²/s found by FHC to yield the best results in their modeling simulations. Given the similarities between the fundamental governing equations used in the model and the FHC model, a value of $N_v = 0.03$ m²/s was first used in the model along with $c_b = 0.001$ m/s as suggested in the previous section. Though the results of the model indicated currents of the right order of magnitude in the vicinity of Buccaneer, currents in the deeper grids were in excess of 7 m/s — a value considered unrealistically high. The reason for this is apparently linked to the fact that depths in the model grid ranged from 7 to almost 200 m. For depth variations of this order, a constant $N_v$ would seem inappropriate since, in the shallower waters, the mixing length and hence $N_v$ are restricted by the water depth. Thus, there is good reason to believe that $N_v$ should be a function of at least the water depth. It is interesting to note that the effect of depth on $N_v$ is not included in suggested relationships for $N_v$ which appear in Neumann and Pierson, among others.

A relationship for $N_v$ suggested by Townsend (22) was found and applied in subsequent modeling. This expression relates $N_v$ to depths in the following manner:

$$N_v = \frac{W_* H}{IR} \qquad (9)$$

where:

IR — the flow Reynolds Number. Townsend suggests a value of 13 for open channel flow.

$w_*$ — the surface friction velocity, $\{(\tau_x^2 + \tau_{sy}^2)/\rho^2\}^{\frac{1}{2}}$

H — the local water depth.

The shear velocity, $w_*$, is proporcional to the wind speed and can be used to vary $N_v$ in both time and space, i.e. $N_v(x,y,t)$. However, as a first approximation, $w_*$ can be kept constant and the grid element depth can be used in (9) to calculate $N_v$ for a particular grid element. Thus, $N_v$ calculated in this manner is a function of horizontal space, i.e., $N_v(x,y)$.

### 4.3 *Modeling Results*

Figure 4 shows a comparison of the FHC data (solid curve) to various simulations. The figure shows temporal variations of the currents at 4, 10 and 19 m below still water level at Buccaneer. All data are broken into onshore and alongshore components. A positive alongshore current would be pointed in roughly a northeast direction in Figure 1. Onshore is indicated as positive. The data were originally plotted by FHC in North-South and East-West components. An adjustment of about 50° is needed to convert to onshore and alongshore components and this was done in Figure 4 since it facilitated physical interpretation of the data.

As one can see from Figure 4, the FHC model (dotted-dashed curve) simulates the alongshore component of the velocities nicely, although the comparison deteriorates after 1600 hours. The onshore component is not simulated as well by the FHC model, there being a considerable discrepancy beginning at about 1400 hours.

Case I (dashed curve) in Figure 4 indicates the results from the model (GAL) using $c_b = 0.001$ m/s. The value for $N_v$ was calculated using (9) with a constant $w_* = 0.04$ m/s, corresponding to the maximum wind velocity observed at Buccaneer. A value of $IR = 13$ was used as suggested by Townsend for open channel flow. The water

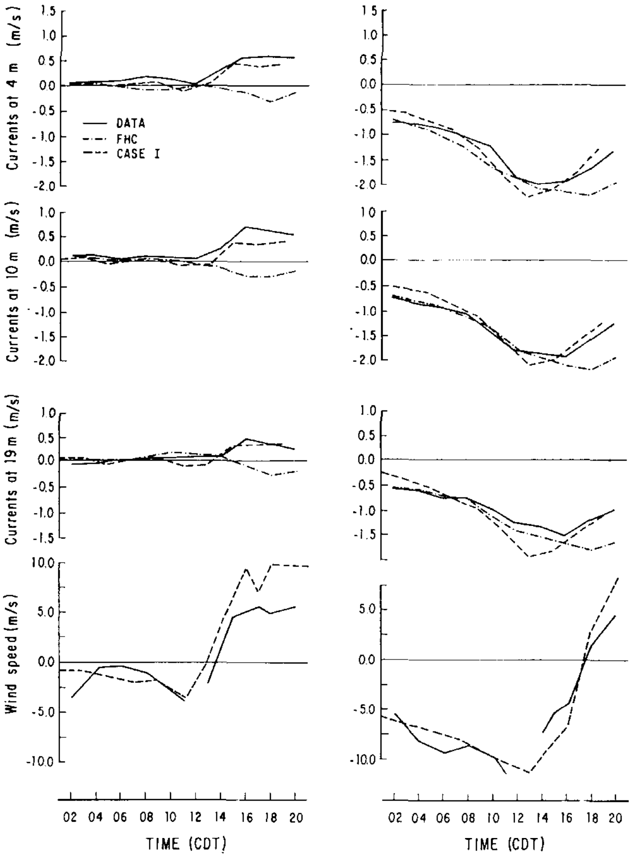


Fig. 4. Comparison of measured currents and winds versus numerical simulation for Tropical Storm Delia (September 4, 1973).

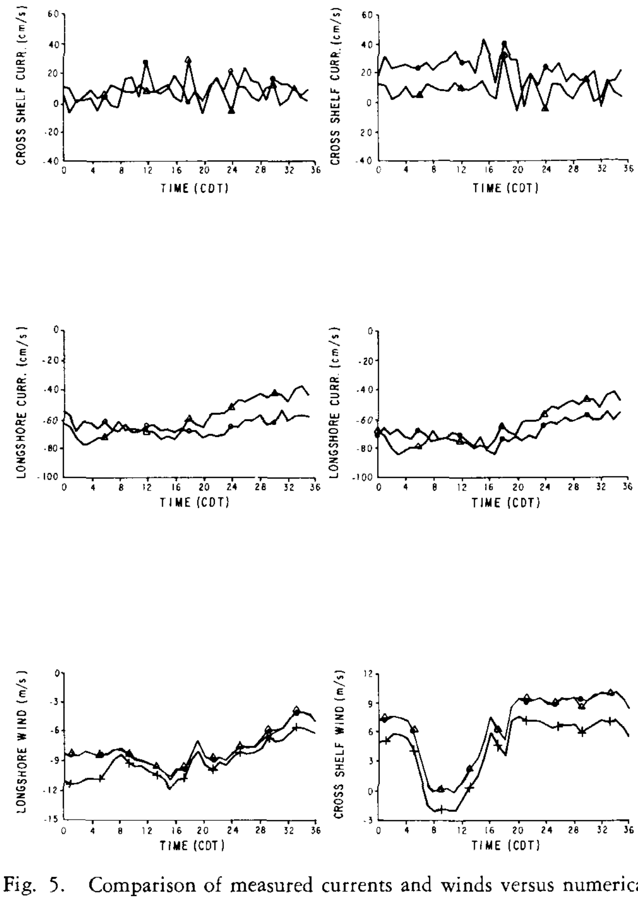


Fig. 5. Comparison of measured currents and winds versus numerical simulation for Hurricane Anita. (September 1st and 2nd, 1977).

depth, H, used in (9) was the local grid element water depth so $N_v$ varied in the model grid between 0.56 $m^2/s$ at the deepest element, H = 183 m, to 0.022 $m^2/s$ at the shallowest element, H = 7 m.

As one can see from the figure, Case I compares well to the data, being within 20% in magnitude, although the peak currents in the simulation precede the observed peak by about 1 to 3 hours. Discrepancies of the order observed lie well within the range attributable to various uncertainties in the modeling process such as the wind field simulations (see lower part of Figure 4 for comparison of winds) or unknown tidal and baroclinic velocity components. The comparison is particularly good in light of the fact that a relatively general method of deriving $N_v$ and $c_b$ was used.

The differences observed between GAL simulations and those of FHC are of interest and the reason for the discrepancies are not obvious. Both models, as applied in the Delia simulation, are founded upon the same basic governing equations and boundary conditions (surface and bottom). The major difference between the two models lies in the solution technique. For mathematical convenience, FHC separate the effects of pure drift from the surface slope. The former problem is solved analytically by means of a convolution integral while the latter is solved numerically by means of a finite difference, vertically averaged model. To get the total current at a particular point of interest, the currents from the two components are summed. Other possible reasons for the discrepancy are: (1) differences in the wind models used or (2) the use of $N_v \neq N_v(x,y)$ in the FHC simulations.

## 5. HINDCASTS OF CURRENTS FOR HURRICANE ANITA

The current data described by Smith (4) was recorded by two ENDECO recording current meters located at 2 and 10 m above the bottom in approximately 17 m of water. Wind velocity was recorded at Port Aransas, approximately 120 km away from the site. Winds were modeled as described in Section 2 and the wind data was input into GAL.

The best fit simulations of currents are shown in Figure 5 using $C_b$ = 0.00025 m/s and (9) for $N_v$. A value of IR = 12 was found to yield good results as was the case for Delia. In general the comparisons are quite good, being within 10 cm/s most of the time.

## 6. DISCUSSION OF HINDCAST

It was found in both hindcasts that current simulations were not very sensitive to changes in $N_v$. For example, if $N_v$ was increased by a factor of 4, the currents decreased by less than 10%, in general. However, currents were very sensitive to changes in $c_b$. For instance, an increase in $c_b$ of a factor of 2 would increase currents by roughly a factor of 2. The sensitivity of currents to $c_b$ is quite significant. The factor of 4 between $c_b$ for Delia (0.001 m/s) and $c_b$ for Anita (0.00025) is important and the reasons for the difference must be resolved if GAL is to be used successfully in a fully predictive mode. To see this imagine that current data did not exist for Anita and that we were simply going to predict currents. A reasonable choice of $c_b$ would be 0.001 m/s given the likely similarities in bottom conditions at the two sites, However, use of $c_b$ = 0.001 m/s for Anita would yield simulated currents roughly a factor of four smaller than those actually observed. Thus, it is important to determine what causes the $c_b$ for Delia to be much higher than $c_b$ for Anita.

Grant and Madsen (23) suggest that the presence of wind generated waves can significantly increase the apparent bottom shear stress in shallow water (high bottom shear stress would be indicated by a large $c_b$). Cooper and Pearce (24) recently tested this hypothesis for the case of Tropical Storm Delia and concluded that the rather large bottom shear stress observed in the data was probably due to surface wind wave activity.

The paragraph above suggests a possible explanation for the much higher $c_b$ observed in Delia than for Anita—the waves were simply larger for Delia. Wave observations for Anita are not available but a hindcast of waves using a simple parametric model by Ross (25) indicates wave heights of about 3 m at the current meter site. Waves observed during Delia reached 8 m in height. Therefore, at least qualitatively, it would appear that the differences in $c_b$ could be explained by the differences in wave activity.

Further studies are presently under way to quantitatively verify the above hypothesis. The model proposed by Grant and Madsen will be used to take into account the effects of waves on $c_b$. The work is not only important for modeling on the Venezuelan coast but it is also of importance for modeling elsewhere using other types of circulation models.

## 7. CONCLUSIONS

The simulations described above verify the model capability to accurately hindcast currents generated by tropical storms. Further studies are being undertaken to define better the physical processes affecting $c_b$ and $N_v$. It seems apparent at this point that waves will significantly influence $c_b$.

Once the factors affecting $c_b$ and $N_v$ have been more adequately quantified, it will be possible to apply the model to any site in order to predict storm generated currents and other circulation characteristics.

## 8. ACKNOWLEDGMENTS

Mr. Edward Doyle, a graduate student at the University of Maine, performed the preliminary simulations for Tropical Storm Delia and the simulations for Hurricane Anita. Prof. Bryan Pearce was also involved in those simulations. Mr. Ned Smith of Harbor Branch Foundation Inc., provided the original time series of current data collected during Anita.

## REFERENCES

1) PEARCE, B. R.; COOPER, C. K. Numerical Model for Wind-Induced Flow. *Am. Soc. Civ. Eng., Hydraulic Division.* In press. Fall 1980

2) PEARCE, B. R.; COOPER, C. K; DOYLE, E. Hurricane Generated Currents *Proc. Conf. Civ. Eng. Oceans IV, Am. Soc. Civ Eng* San Francisco September 1979

3) FORRISTALL, G. Z.; HAMILTON, R. C.; CARDONE, J. V. Continental Shelf Currents in Tropical Storm Delia: Observation and Theory. *J. Phys. Oceanogr.* 1977. 7 (4) : 532-546.

4) SMITH, N. P. Longshore Currents on the Fringe of Hurricane Anita. *J. Geophys. Res.* December 20, 1978. 83 (C12) : 6047-6051.

5) HARRIS, D. L. Meteorological Aspects of Storm Surge Generation. *Am. Soc. Civ. Eng., Hydraulic Division.* 1958 HY7. 25 p

6) STONE AND WEBSTER ENGINEERING CORP. *Determination of Coastal Storm Tide Levels*, Boston. October 1978.

7) JELESNIANSKI, C. P. Splash - Special Program to List Amplitudes of Surges from Hurricanes. *Nat. Oceanic Atmos. Adm. (U.S.)*.

8) MYERS, V A ; MALKIN, W. Some Properties of Hurricane Wind Fields as Deduced from Trajectores. *U.S. Dep. Commer.* 1961. Report Nº 49

9) WU, J. Wind Stress and Surface Roughness at the Air-Sea Interface *J. Geophys. Res.* 1969. 74: 445-455.

10) CARDONE, V. J.; PIERSON, W. JR,; WARD, E. G. Hindcasting the Directional Spectra of Hurricane Generated Waves. *J. Pet. Technol.* 1976 18:385-394

11) CARDONE, V. J. Specification of the Wind Distribution in the Marine Boundary Layer for Wave Forecasting. *Geophysical Sciences Laboratory, New York University.* New York. 1966.

12) HEAPS, N. S. On the Numerical Solution of the Three-Dimensional Hydrodynamic Equations for Tides and Storm Surges. *Mem. Soc. R. Sci. Liege* 1972 6 (2): 143-180

13) HEAPS, N. S. Development of a Three-Dimensional Model for the Irish Sea. *Rapp. P.V. Reun. Cons. Inst Explor Mer* December 1974: 147-162.

14) GULDBERG, C. M., MOHN, H. Etudes sur les Mouvements de L'atmosphere. 1876 (revised 1883-1885). Christiania Translation by Cleveland Abbe. *Smithsonian Misc. Coll.* Washington, D C 1910 3: 122-248

15) WANG, J. D ; CONNOR, J J Mathematical Modeling of Near Coastal Circulation. *R. M. Parsons Lab. Water Res. Hydro., M.I.T.* 1975 TR200.

16) WEARE, T. J. Finite Element or Finite Difference Method for the 2-D Shallow Water Equations. *Comput. Methods Appl. Mech. Engr.* 1976. 7: 351-357.

17) DAILY, J. W.; HARLEMAN, D. R. F. *Fluid Dynamics*, Reading, Massachusetts: Addison-Wesley, 1966.

18) NEUMANN, G.; PIERSON, W. *Principles of Physical Oceanography.* New Jersey: Prentice Hall Inc., 1966; 545 p

19) SCHMIDT, W. Wirkungen der ungeordneten Bewegungen im Wasser der Meere und Seen. *Ann. d. Hydr. u. Marit. Meteorol.* 1908. 45: 367-381 and 431-445.

20) THORADE, H Die Geschwindigkeit von Trifstromungen und die Ekman'sche Theorie *Ann. d. Hydr. u. Marit. Meteorol* 1914 42: 379

21) NEUMANN, G On the Complex Nature of Ocean Waves and Growth of the Sea under the Action of Wind. *Gravity Waves, N.B.S. Circular,* 1952 p 521

22) TOWNSEND, A A *The Structure of Turbulent Flow*, Cambridge University Press, 1976; 429 p

23) GRANT, W. A.; MADSEN, O. S. Combined Wave and Current interaction with a Rough Bottom *J. Geophys. Res.* 1977 84 (C4).

24) COOPER, C. K.; PEARCE, B. R. On the Forcing Mechanisms Affecting the Bottom Shear Stress in Coastal Water. *J. Phys. Oceanogr. In Press. Fall* 1980.

25) ROSS, D B Simplified Model for Forecasting Hurricane Generated Waves. *Bull. Am. Meteorol. Soc.* January 1976.

*Recibido: 10-9-80*
*Aprobado: 28-9-80*